Machinability of PA12 and short fibre–reinforced PA12 materials produced by fused filament fabrication

Isaac Ferreira[1,2] · Rui Madureira[1] · Santiago Villa[1] · Abílio de Jesus[1,2] ·
Margarida Machado[2] · Jorge Lino Alves[1,2]

Abstract

Fused filament fabrication (FFF) is an extrusion-based process that allows quick and inexpensive part production, practically without any geometric limitations, offering flexibility, promoting reduction in costs and lead-time in an industrial scenario. Being one of the most widespread additive manufacturing techniques, the process has evolved introducing new and advanced materials (e.g. high-performance polymers and composites). Despite its advantages, the process is vastly overlooked due to its high level of anisotropy, poor surface roughness and lack of geometric accuracy caused by the layer thickness. To reduce this effect, a sequence of laborious manual operations can be performed, which may result in time-consuming and inaccurate results. Therefore, efforts have been made towards the development of hybrid manufacturing technologies by combining FFF process and subtractive equipment, aiming to solve these limitations. In this work, two complementary methodologies analysing the behaviour of FFF PA12 and short fibre–reinforced PA12 printed parts when subjected to a subtractive approach are presented. The first experimental plan took into account the final surface roughness (Ra and Rz) via full factorial design of experiments (DOE) and analysis of variance (ANOVA) considering the influence of distinct printing orientations, two types of cutting tools and machining parameters such as, cutting speed, feed and cutting depth. An analysis on tool wear and SEM microscopy to the machined surface was also performed. The second approach was carried out via Taguchi and ANOVA, considering the first experimental approach results. Thus, milling parameters were the focus, evaluating the final material surface roughness, being now monitored the cutting forces and tool wear analysis in order to understand their influence on the final results. It is shown that it is possible to machine PA12-based FFF printed parts without any major problems such as layer delamination. A decrease in Ra, t of 1931% to 0.99 μm for PA12CF and 2255% for PA12 to 0.96 μm was achieved, proving the overall machinability of the materials. It was found that PA12 creates higher levels of cutting loads and increased tool wear, thus indicating that short fibre presence improves the material machinability, while parameters such as building orientation do not possess any influence on the final surface roughness.

Keywords FFF · Additive manufacturing · Hybrid manufacturing · Composites · Composite machining

1 Introduction

Advances in additive manufacturing (AM) stand for a new era in fabrication, resulting in a fresh way of thinking, how people imagine and design parts for production. Due to its layer-by-layer approach, AM opens fabrication possibilities that conventional processes cannot respond to. Even though this process was initially intended for prototyping purposes, the subsequent evolution that the distinct techniques have been subjected to, opened the path for consumer ready parts. ISO/ASTM 52900:2015 [1] divides AM technologies into seven distinct categories, among them, material extrusion, powder bed fusion, material jetting, binder jetting, direct energy deposition, sheet lamination and vat polymerization. All of these methods use similar approaches to part production, from the CAD model, to the parametrization selection and toolpath generation in slicing, beyond layer wise production and finishing post-processing.

One of the most popular additive technologies, is commonly known as fused filament fabrication (FFF), which is inserted in the material extrusion branch. This technique consists into the liquification of a thermoplastic-based material,

✉ Isaac Ferreira
   iaferreira@inegi.up.pt

Extended author information available on the last page of the article.

by raising its temperature and extruding it through a small diameter nozzle. Then the desired shape is created layer-by-layer, quickly solidifying the material by decreasing its temperature due to its contact with the surrounding air and the previously deposited material layers. FFF was one of the most widespread technologies in early 2000 for polymeric materials, becoming one of the broadest processes offering from the low-cost to high-end industrialized equipment cost-effective solutions. With the evolution of technology, new material formulations were developed and a vast list of possible processable materials shows the technology's potential. Polylactic acid (PLA), the acrylonitrile butadiene styrene (ABS) and the polyethylene terephthalate glycol (PETG) may be defined as the most common materials, followed by the engineering polymers such as Polyamides (PA), Polycarbonates (PC) and high-performance, high-temperature polymers (i.e. Polyether ether ketone (PEEK) and Polyether Imide (PEI)). However, this meant that the hardware had to follow this evolution, fulfilling the material processing requirements. The creation of these high-performance materials was motivated by the usual low mechanical properties of the raw material. Following, this same evolution, composite materials have been adapted to the process being currently an important variant of the technology. With the addition of short fibres, nanotubes or continuous reinforcements to traditional matrix materials such as PA and PETG, an improvement in the final part mechanical behaviour has been achieved. Without these high-performance materials/composites, the process would still not be considered as a significant alternative by the industry, thus creating the possibility of new applications in aerospace [2, 3], automotive [4], sports [5] and health [6].

Even though the advantages presented by the process, there are several challenges when facing other AM technologies. FFF parts present a higher level of anisotropy, partly due to the thermal residual stresses caused by successive heating/cooling cycles and its higher layer thickness. As a consequence of that layer thickness, the process typically originates poor surface finishing (e.g. pronounced staircase effect due to the rounded geometry of the deposed line [7]). These issues tend to be accentuated for higher extrusion diameters or higher layer thicknesses as in big dimension parts. The thermal gradient created by the continuous material deposition can also influence the part dimensions, as well as the interlayer adhesion strength, since it dictates the type of connection between the adjacent layers [8]. Moreover, the sequence of thermal cycles to which the material is subjected to, from polymeric expansion after leaving the nozzle, to the posterior shrinkage induced by the material cooling, create a unpredictable lack of precision and consequent poor geometric accuracy. Taking into account the process capabilities such as the wide range of materials, properties

and low cost, the technology is now evolving towards the hybrid sector, where a machine can print and correct the part dimensions and surface quality via subtractive manufacturing.

Several studies have been developed in order to investigate the dimensional accuracy of FFF printed parts. Santana et al. [9] studied the influence of layer thickness, infill density, deposition speeds, extrusion temperature and extrusion multiplier on the part dimensional accuracy in *xyz* directions. Through Taguchi method and ANOVA statistical analysis, it was possible to conclude that the infill density and extrusion multiplier are the most influential factors, being responsible for the printed samples distortions. Sood et al. [10] analysed the influence of part orientation, raster width, layer thickness, air gap and raster angle on dimensional accuracy. By applying the Taguchi method, it was found that sample shrinkage was the most critical defect, since specimens were smaller in every direction. A final set of ideal parameters were developed according to the statistical data analysis, reducing this phenomena. Zhang and Peng [11] applied the same method in an equipment with fuzzy logic and analysed parameters as raster width, layer thickness, infill speeds and printing speeds. It was concluded that the most influential factor was raster width, followed by printing speed, layer thickness and infill speeds. Dimensional accuracy is also a consequence of the feedstock intrinsic properties; therefore, its prediction is only possible through the complete characterization of the materials to be tested.

FFF is one of the additive processes that presents the weakest surface finishing. The surface of the final part depends upon how thin the layer thickness is, which is especially problematic in large volume parts. Higher levels of detail lead to increased print times and consequently higher costs. Low-detail parts often require manual labour, which can be an imprecise and time-consuming operation. Beyond the manual treatment, chemical finishing and machining methods for improving final part quality have been studied. Galantucci et al. [12] researched the link between FFF process parameters and surface roughness in a first step, and posteriorly tested the chemical bath finishing (acetone) on ABS-printed parts. Singh et al. [7] also evaluated chemical (acetone) exposition technique via vapour smoothing station on parts roughness. A design of experiments (DOE) was carried out in order to identify the most influential parameters on the surface finishing. It was shown that surface finish was improved to nano-level without deviating from the initial dimensions. There have been several studies regarding ABS-printed parts acetone bath/vapour smoothing techniques showing promising results [13, 14]. However, the finishing process using acetone is only possible for ABS and is extremely complex to control.

Machining a FFF-printed part creates the possibility of benefiting from the accuracy provided by the subtractive process. The downfall of this technique is the need of specific hardware and all of the pre-machining routines involved in the process. As AM is the process of creating parts by adding layers of material upon itself, subtractive processes implicate the use of several techniques and processes into a piece of raw material, removing it until the desired shape is created. Since there is the need of post-processing FFF-printed parts with inadequate dimensional accuracy and surface quality, further investigation towards the development of hybrid techniques is necessary, combining the material deposition with subtractive operations in a single machine. In a novel approach, Amanullah et al. [15] developed a hybrid setup capable of both types of fabrication. This machine was composed by a FFF extruding head and a CNC cutting spindle in a cartesian three-axis kinematic, capable of one extra movement by rotating the tool plate (CNC spindle/extruder) embedding both technologies with a single control panel. Lee et al. [16] have shown prominent results in the development of an hybrid five-axis machine equipped with a rotating plate composed by a FFF extruder in one side and the spindle in the other. Case studies showed that by using a hybrid technique, the building time was reduced upwards 50%.

Considering this approach, machining parameters for printed parts need to be investigated. Since the parts are not made from a homogeneous block of material, the existing recommended parameters for polymeric solid materials are just a starting point. Beyond the influence of the printing process parameters and the material, the subtractive component presents challenges at parameters and tools selection. Boschetto et al. [17] addressed this topic by printing according to several deposition angles, square parallelepiped ABS samples, and posteriorly measuring surface roughness for different cutting depths for each sample. In a study developed by Tomal et al. [18], a combination of FFF with abrasive milling was used to improve the dimensional accuracy and surface finish. The results showed an improvement in dimensional accuracy from 71 to 99% when comparing the original part with the milled one. In addition, the surface roughness (*Ra*) was measured presenting an improvement up to 91.3%.

To the best of the author's knowledge, studies conducted earlier focused on face milling as the finishing technology are dedicated to more traditional materials such as ABS and PLA [17, 18], considering fewer machining parameters (e.g. cutting depth, feed and cutting speed), aiming at improving surface roughness. In regard metallic materials, subtractive processes have been widely used for surface roughness enhancement. As shown by Kara et al. [19, 20] and Karabatak et al. [21], distinct process parameters were analysed, the Taguchi method coupled with ANOVA analysis being applied to obtain a combination of parameters allowing for an improved final surface roughness. Similarly to the above-mentioned researches, it is initially intended in this study to create the parameters window for a machining operation. For such purpose, the face milling operation is considered in machining both Polyamide 12 (PA12) and short fibre–reinforced PA12 (PA12CF) printed parts are considered, taking into account that the abrasiveness of fibre reinforcement might present a challenge for the cutting tools. This study is seen by the authors as a required step to understand the behaviour of FFF parts when subjected to subtractive operations, leading the way towards the development of hybrid technologies possibilities. It is a purpose to allow the application of developed methodology in this study to other materials so that the adequate machining parameters may be obtained.

This paper is structured as follows: an introductory section addresses the FFF state-of-the-art, afterwards, a section presenting the materials and the additive production details which are common for both approaches. The research approach is divided into two major sections, representing the first and second approach. In each section, the experimental methods that describe the procedure are explained, followed by the results and discussion, being complemented by a final summary. Lastly, final conclusions concerning the whole work are presented.

2 Materials and specimens production

2.1 Materials

The material selection for this study consisted of two versions of Polyamide 12 (PA 12) ⌀ 1.75-mm filament from Fillamentum©, Parzlich s.r.o (Czech Republic). PA 12 - Nylon FX256 [22] from now on referred as PA12 and PA12-Nylon CF15 [23] (referred as PA12CF) as the reinforced version of the first brand. As indicated by the manufacturer datasheet, PA12CF is reinforced by 15 wt% of short carbon fibres with 100 μm in length and 10 μm in diameter. Table 1 depicts some of the relevant material

Table 1 Datasheet values and material specifications [22, 23]

Property	CF15	FX256
Material density (g/cm^3)	1.08	1.01
Melt flow index ($g/10min$)	14.64	16.56
Glass transition temp. T_g (°C)	44.70	52.91
Thermal conductivity (10^{-3} W/m.k)	144.22	124.82
Tensile strength (MPa)	54.50	45.00
Tensile elastic modulus (MPa)	500	1400
Melting temperature (°C)	160	178
Print temperature (°C)	235–260	235–260

properties. This type of polymer is largely considered as an engineering thermoplastic, being suited for several load bearing applications. Its properties also include a high-elastic modulus, as well as improved tensile strength, low friction coefficient and wear resistance. The application of this type of materials to the FFF technology allows an evolution in mechanical performance of the parts. Furthermore, most of the research in this field, considering the process of FFF, is done with commodity polymers such as ABS and PLA [17, 18]; therefore, it is of the most interest to develop knowledge with these new materials in order to further push the process.

2.2 Sample definition and production strategy

The developed specimen geometry for machinability testing (face milling with end cutters) was defined considering the following influential factors: (i) The machinable face must have a minimal length of 60 mm in one direction, allowing stabilization of the milling process; (ii) Each sample should maximize the number of tests, maintaining easy printability, while reducing material waste; (iii) Since machining trials were performed at surface level, it is important to ensure a near 100% dense at surface level. The choice also took into consideration the tool diameter, the cutting tool overlapping between passes and finally, the printing capacity of the FFF machine. Thus, the selected geometry corresponded to a quadrangular prism with dimensions of 30×30×60 mm (Fig. 1), with fully dense shells (bottom, top layers and perimeters) and internal infill of 15%.

The samples were manufactured in a Tronxy X5 3D printer from Shenzen Tronxy Technology Co. Ltd, and the process planning was performed with Simplify3D®4.0.1. Table 2 lists the parameters used in the production of the samples. The choice of the parameters was based on preliminary tests, which revealed to be the ones that presented increased printability, reduced warping and good visual aesthetics [24].

As previously mentioned, the surfaces to be machined were produced with a fully dense shell. Regardless of the printing orientation, and according to the parameters presented in Table 2, 15 top and bottom layers were needed to achieve the 3-mm machinable surface (0.2-mm layer height). For the lateral walls, the same shell thickness was achieved by using 8 perimeters (raster width of 0.4 mm, as shown in Fig. 1).

3 Research approach

As presented in Fig. 2, this work describes two consequent approaches for the problem of machining FFF printed parts. The first approach is based on a full factorial design
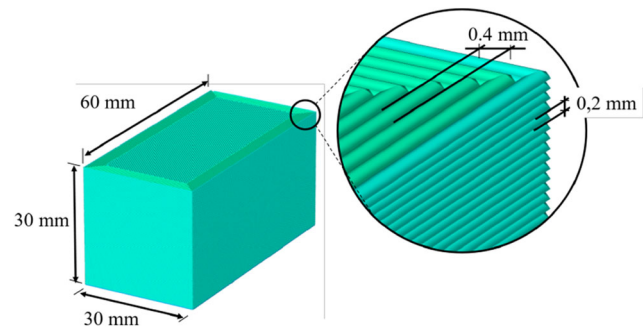

Fig. 1 Sample dimensions and deposition strategy

of experiments (DOE) and respective ANOVA analysis, considering four different types of variables, being those the material, cutting tool, machining parameters and building orientation. With this first approach to the problem, it was possible to create a first set of ideal parameters for optimized roughness. As a result, a second research was undertaken, disregarding some non-influential conditions, but keeping both materials and widening the milling parameter variables in a new Taguchi DOE and statistical analysis. A new machining hardware setup (stiffer, more precise/stable machine) was also considered in order to compare possible machine influence on the final part properties. A multicomponent dynamometer was used for cutting forces measurement. As a result, surface roughness, cutting forces and tool edge microscopic analysis, for each set of variables, were obtained, allowing a better insight of the machining process. This study is seen by the authors as a step needed in the evolution of the process towards the development of a hybrid technique.

Table 2 Fused filament fabrication parameters

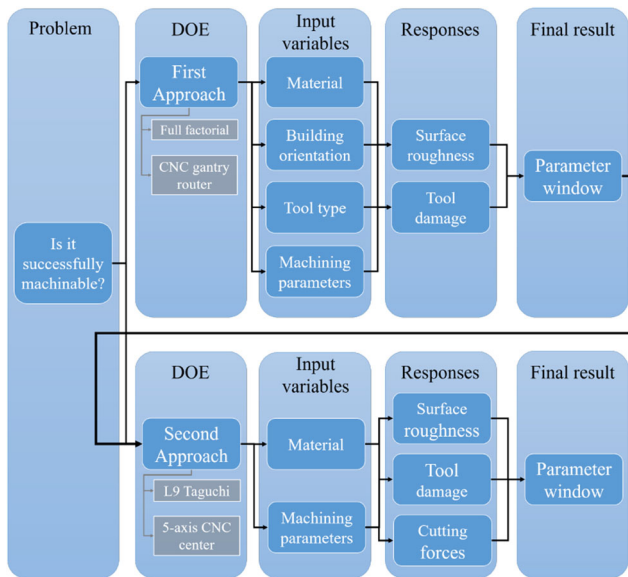| Extrusion parameters	
Nozzle diameter	0.4 mm
Extrusion multiplier	1.05
Layer parameters	
Layer height	0.2 mm
Raster width	0.4 mm
Top/bottom solid layers	15
Number of perimeters	8
Infill pattern	±45°
Infill percentage	15%
Temperatures	
Extrusion temp.	260 °C
Bed temp.	90 °C
Speed	
Printing speed	40 mm/s

Fig. 2 Work plan schematic

3.1 Experimental approach 1

3.1.1 Methods

Within this section, experimental approach 1 is described in detail. The machining test hardware and protocol is presented, as well as the defined DOE and the surface roughness analysis prior and after the machining test. The main goal is to develop a machining parameters window for face milling finishing operations, improving the surface roughness by considering four types of variables: milling parameters (cutting speed, feed and depth of cut), material (PA12 and PA12CF), tool specification (2 or 4 flute) and print orientation.

Subtractive hardware A Ouplan CNC Routers Checkbox 1008 was used. This milling machine presents a cartesian 3 axis gantry structure, with a maximum working size of $1100 \times 850 \times 200$ mm, being capable of displacement speeds up to 25 m/min. It is equipped with a spindle that can

achieve up to 24000 RPM, while the tool clamping is done by an ER-32 type system. This machine is recommended for light work and presents lower stiffness and stability than CNC machining centres as the one to be used in the second experimental approach.

DOE - first test programme In order to combine all of these input values (A-Material, B-Tool, C-Building orientation, D-Cutting speed, E-Feed and F-depth of cut), a full factorial DOE was defined as the basis of this experimental analysis, resulting into ninety six different conditions, as presented in Fig. 3. The experimental data obtained from tests (surface roughness) was investigated via ANOVA in order to identify the truly contributive parameters (using a confidence interval of 95%). This will allow further along the investigation path for a better parameter combination choice considering the obtained responses.

Building orientation: Concerning building orientation, horizontal specimens were produced at 0°, tilted at 45°, with support structures and upright position at 90°, as shown in Fig. 4. By testing these three types of samples, it is possible to investigate how influential can the deposition orientation be on the machining process, since the tool will intersect shell lines deposed perpendicularly, parallel and 45° to its travelling path.

Tool: Regarding the tool choice, two types of ∅ 8 mm solid carbide end-mills supplied by Palbit, S.A. were used. A flat end two flute tool without coating, with an helix angle of 14° (HFMA200820-SOFTLINE) (Fig. 5a) was selected. The second type was a flat end four flute tool, with 30° of helix angle and a diamond coating (HF30A400815 R050-KOPIEFR LINE) (Fig. 5b). Both tools were subjected to two levels of three machining parameters, namely cutting speed, feed and depth of cut. The full set of experiments was performed using only two tools (one of each type).

Cutting parameters: Prior to the first experimental plan, exploratory tests were performed by submitting the

Fig. 3 Approach 1 - Full Factorial DOE test matrix
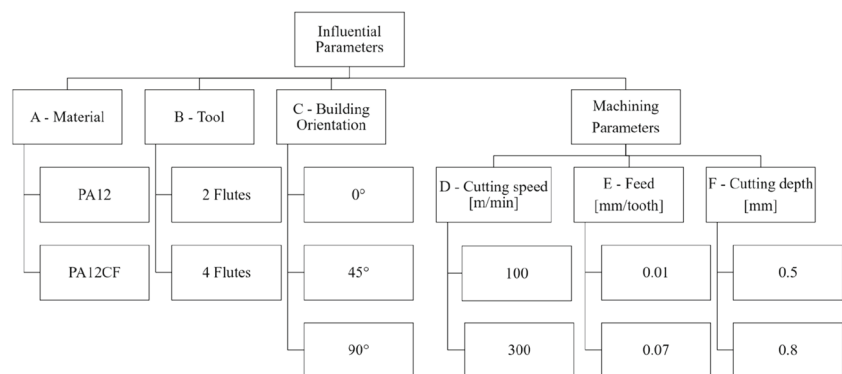
Fig. 4 Distinct building orientations. **a** 0°(horizontal/flat position), **b** 45° (tilted position) with support structures generated by the Simplify3D software and **c** 90° (upright position)
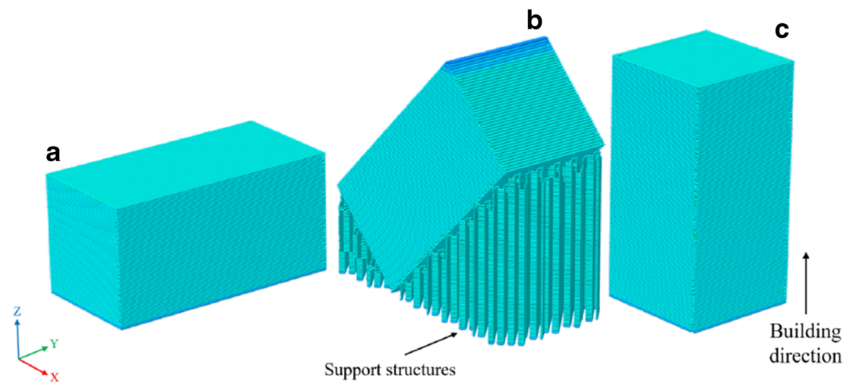
samples to a wide range of cutting speeds, based on the literature recommendation summarized in Table 3, defining a first estimate window for cutting parameters. Considering this first analysis, cutting speed values process range were defined between 100 and 300 m/min, while the feed per tooth was 0.01 and 0.07 mm/tooth, the chosen cutting depth of 0.5 and 0.8 mm.

Machining strategy: Considering the high number of samples needed to accomplish the full factorial DOE, each face of the testing specimen was divided into two sectors and machined (end face milling) with a different set of cutting parameters, as illustrated in Fig. 6. With this machining tool routine, an overlap of 2 mm between paths is observed, which corresponds to 25% of the tool diameter. The machining strategy was created via Mastercam Mill X9©.

Material and tool analysis

Roughness measurement: The specimens surface roughness was measured using a profilometry Hommel-werle with a TK 300 tip (LV-50) with a diamond needle of ±300 μm. The analysis was performed at an average
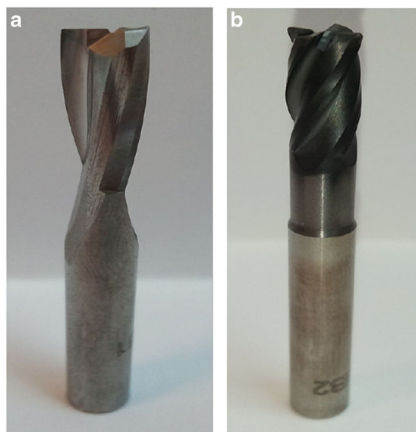
Fig. 5 Cutting tools. **a** Flat end two flute and **b** flat end four flute tool

speed of 0.5 mm/s for a total measuring length of 4.8 mm, according to ISO 4288 [29]. For each specimen the surface roughness was assessed three times along two orthogonal directions: Ra, l (longitudinal) and Ra, t (transversal). Ra which is normally referred as roughness is characterized by the arithmetic mean of the ordinate's absolute (height values) within a base length. For comparison purposes, the measurements were taken prior and after the machining operation, as presented in Fig. 7. It is important to consider that Ra, l is measured in the machining feed/path direction, while Ra, t is across the machining path.

SEM analysis: Scanning electron microscopy testing was performed in the machined samples using a Quanta 400FEG ESEM/EDAX Genesis X4M in order to understand the surface morphology of distinct processing variables combinations, fibre behaviour and polymer/fibre interaction.

3.1.2 Results and discussion - experimental approach 1

Pre-machining surface roughness Table 4 depicts the roughness analysis results carried out prior to specimen machining. It is possible to observe a relationship between building orientation and Ra, l and Ra, t. Horizontally built samples (0°) present higher Ra, t than Ra, l for both materials, indicating that longitudinal measurements were made along the layers/deposition lines. The opposite behaviour is found for the upright samples (90°) in which longitudinal measurements are made perpendicularly to the layer deposition. For the tilted samples (45°), surface roughness is similar both longitudinally and transversally, since the measurement is done at 45° to the deposition direction. Therefore, it can be concluded that a 0.2-mm layer height leads to an average (perpendicular measurements to the deposed lines) roughness of 19.55±5.12 μ for PA12 and 19.01±0.25 μm for PA12CF.

ANOVA - approach 1 Table 5 presents ANOVA results for the transversal roughness (Ra, t) analysis. Considering

Table 3 Literature overview for cutting parameters for polymer machining

| Material	Type of tool		Cutting parameters					Reference
	Type/Material		Diameter (mm)	Cutting flutes	Cutting speed (m/min)	Feed (mm/tooth)	Cutting depth (mm)	
PA66, PA66-GF30 PA66-MoS2	Solid carbide inserts		121	8	186 to 294	0.100 to 0.157	1.00 to 1.56	[25]
PEEK	Solid carbide end mill		10	2	126 to 251	0200 to 0.300	4.00 to 8.00	[26]
PA6G	End mill and solid carbide end mill		10, 14 and 18	4	100 to 140	0.008 to 0.015	1.00 to 2.00	[27]
CFRP	Solid carbide inserts		25	2	160 to 200	0.015 to 0.050	6.75	[28]
ABS – P400	Solid carbide end mill		6	2	156 to 360	0.025	0.05 to 0.50	[17]
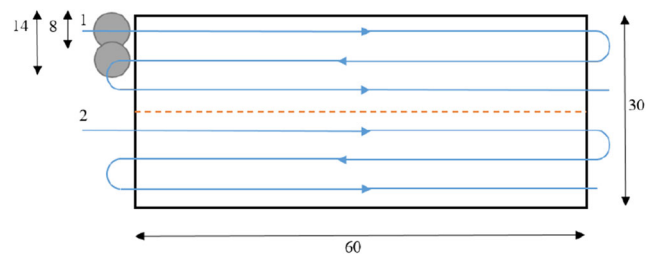
Fig. 6 Machining strategy for the first methodology with two distinct parameter sets applied to each face

the above-mentioned confidence interval (95%), if the P value is higher than 0.05, the parameter or combination of parameters is considered as non-influential to the final results, and consequently not presented in the model.

Building orientation and depth of cut do not show relevant influence on roughness results, nor some interactions between these parameters. From the remaining four input parameters, the results show that the more significant one is the material with the highest contribution of 13.78%, followed by cutting speed (11.76%), then the feed (2.79%) and finally the tool with 2.76% of contribution, in a total of 31.09% of importance. There are six interactions presenting a total contribution of 51.42%, thus indicating the importance of the parameters combination, with the cutting speed/feed (D-E) being the most important (15.27%), followed by tool/feed (B-E) (13.17%), tool/cutting speed (B-D) (11.45%), material/tool (A-B) (5.51%), material/cutting speed (A-D) (4.75%) and finally material/feed (A-E) (1.27%). It is worth noting that some of these interactions present greater influence on Ra, t than each parameter alone.

Through the main effects plot analysis in Fig. 8, it is observable the influence of independent input variables.
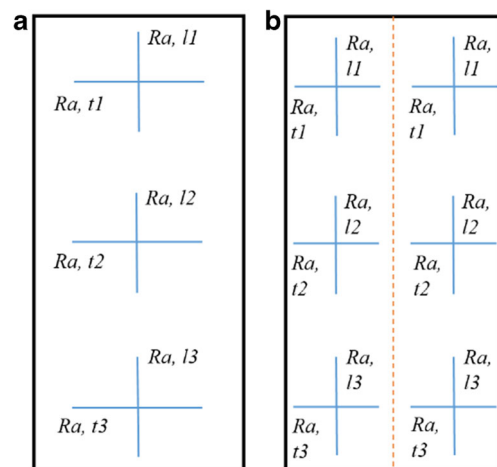
Fig. 7 Measurement points for Ra, l and Ra, t. Prior (**a**) and after (**b**) machining

Table 4 Surface roughness prior to machining tests (average values with standard deviation)

Building orientation (°)	Material	$Ra,t(\mu m)$	$Ra,l(\mu m)$
0	PA12CF	19.12 ± 1.96	3.83 ± 0.53
45	PA12CF	16.88 ± 3.86	16.63 ± 4.30
90	PA12CF	6.13 ± 2.14	18.89 ± 1.61
0	PA12	21.65± 2.90	2.45 ± 6.19
45	PA12	13.63 ± 8.50	13.76 ± 3.38
90	PA12	2.61 ± 5.77	17.45 ± 10.14

It can be perceived that the best transversal roughness is obtained with PA12CF material, processed with a two flute tool, a cutting speed of 100 m/min and a feed of 0.07 mm/tooth.

Figure 9 presents the transverse roughness fitted interactions, with interactions, B-D, B-E and D-E as the most contributive ones. For B-D, the 2 flute tool presents similar Ra,t for both cutting speeds; however, the 4 flute tool presents better surface roughness with lower cutting speeds 100 m/min, while at 300 m/min the roughness is higher. B-E interaction indicates a better behaviour for the two flute tool at lower feeds, increasing the surface roughness for higher feeds (0.07 mm/tooth), while the 4 flute tool presents roughly the same behaviour at higher feeds than the two flute tool at lower values. Finally, D-E, proving to be the most influential one, shows that at 0.07 mm/tooth (feed) the behaviour is roughly similar for both cutting speeds, while at lower feeds (0.01 mm/tooth) surface roughness is worst with the increase in the cutting speed from 100 to 300 m/min.

For longitudinal roughness (Ra,l), Table 6 depicts the results considering the same statistical analysis for the transverse roughness. In accordance with the Ra,t

Table 5 ANOVA Ra,t results (1st experimental approach)

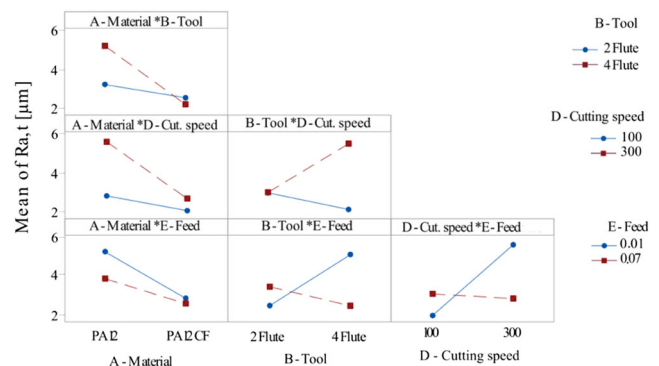| Source	DF	SS	Contribution	F-Value	P-Value
A - Material	1	80.14	13.78%	71.18	0.000
B - Tool	1	16.05	2.76%	14.25	0.000
D - Cutting Speed	1	68.39	11.76%	60.75	0.000
E - Feed	1	16.21	2.79%	14.40	0.001
A-B	1	32.03	5.51%	28.45	0.000
A-D	1	27.64	4.75%	24.55	0.000
A-E	1	7.38	1.27%	6.55	0.012
B-D	1	66.55	11.45%	59.11	0.000
B-E	1	76.59	13.17%	68.03	0.000
D-E	1	88.80	15.27%	78.87	0.000
Error	85	93.45	17.47%		
Total	95	581.37	100%		
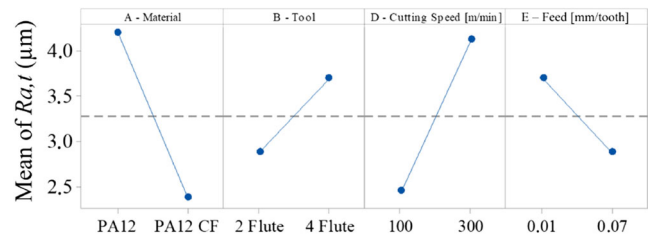
Fig. 8 Main effects plot for Ra,t

ANOVA's results, building orientation and depth of cut are not influential, nor the relative combinations. The independent parameters analysis, shows the feed as the most important contribution in this case (10.68%), followed by material (8.92%), cutting speed (8.86%) and the tool (1.59%), with a total contribution of 30.05%. Two way interactions present 47.04% and the most important contribution being the tool-feed (B-E) (17.84%), followed by cutting speed-feed (D-E) (14.24%), tool-cutting speed (B-D) (7.15%), material-feed (A-E) (3.75%), material-cutting speed (A-D) (2.24%) and finally material-tool (A–B) with 1.82% contribution. However, the error value is higher in longitudinal roughness results than what was presented in Table 5.

Main effects plot for Ra,l (Fig. 10) shows that the ideal combination of parameters are in concordance with the ones obtained for the previous measurements. However, the major contribution is given by the feed (10.68%), contrasting with the 2.79% for Ra,t, with the optimal value not as low as in transverse direction.

By comparing the two way interactions on Fig. 11 for the transverse roughness, it is possible to observe that the trend is kept with very few differences. Once again, the three most influential interactions are B-D, B-E and D-E, which are the same most influential combination in transversal roughness results. Considering B-E, which is the most statistically contributive (17.84%) interaction, it is possible to observe that for both speeds result in similar roughness for the two flute tool. The four flute tool presented improved

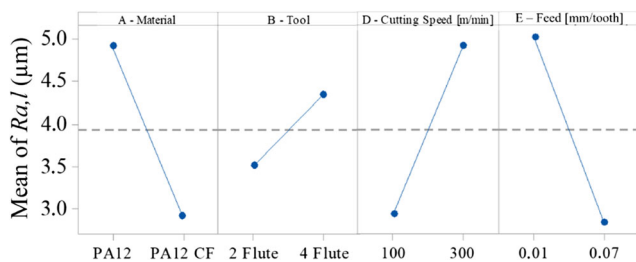

Fig. 9 Two way interaction plot for Ra,t

Table 6 ANOVA *Ra,l* results (1st experimental approach)

Source	DF	SS	Contribution	*F*-value	*P* value
A - Material	1	95.72	8.92%	33.10	0.000
B - Tool	1	17.02	1.59%	5.89	0.017
D - Cutting speed	1	95.00	8.86%	32.85	0.000
E - Feed	1	114.63	10.68%	36.64	0.000
A-B	1	19.48	1.82%	6.74	0.011
A-D	1	24.00	2.24%	8.30	0.005
A-E	1	40.25	3.75%	13.92	0.000
B-D	1	76.76	7.15%	26.54	0.000
B-E	1	191.42	17.84%	66.20	0.000
D-E	1	152.71	14.24%	52.81	0.000
Error	85	245.26	21.87%		
Total	95	1072.77	100.00%		

Fig. 11 Two way interaction plot for *Ra,l*

roughness at lower speeds (100 m/min), while a worst response is shown for 300 m/min. Once more, for D-E interaction (second most important at contribution level), there is no significant difference in roughness at lower cutting speeds, despite that at higher cutting speed. For high feeds, the roughness is slightly improved, contrasting with lower values.

Considering the above-mentioned factors, Fig. 12a presents the *Ra,t* comparison of a PA12 CF, horizontally printed, prior and after the machining process with a two flute tool, cutting speed of 100 m/min, feed of 0.01 mm/tooth and cutting depth of 0.8 mm. An improvement is shown in transverse roughness from a 16.45±0.78 to 1.84±0.01 μm. Figure 12b presents the *Ra,l* comparison for PA12 CF, printed tilted at 45°, prior and posterior to machining process with a four flute tool, cutting speed of 300 m/min, feed of 0.07 mm/tooth and cutting depth of 0.8 mm. It is possible to identify an improvement in longitudinal total roughness from a 14.97±1.28 to 1.70±0.30 μm.

SEM analysis Figure 13 depicts SEM results for a vertically printed PA12 CF sample after machining. Figure 13a presents three distinct areas, being the left side the end

of the first parameters' set (check Fig. 6); the right side shows the beginning of the second parameters' set, and the centre, which is marked with a white circle, it clearly shows the overlap area of the previous passes. Both paths were machined with a four flute tool, with a speed of 100 m/min and a cutting depth of 0.8 mm, however, in the left side (parameter set 1) the feed was 0.07 mm/tooth while in the right side a 0.01 mm/tooth was used (parameter set 2), presenting *Ra,l* values of 1.54±0.10 and 2.52±1.02 μm respectively, confirming the trend indicated in Fig. 10. However, by analysing the Tool-Feed interactions it is possible to conclude that four flute tools require an higher feed to produce better roughness. This effect is seen for Ra, l and Ra, t. Lower feed rates, indicate lower displacement per tooth, thus, presenting a difference in behaviour for two and four flute tools. By imposing an higher number of rotations in the same area, could increase the sample's temperature and lead to irregular material removal. Figure 13b and c depict local magnifications of both machining parameter sets. Figure 13b exhibits a smoother surface, with diminutive fibre presence, thus
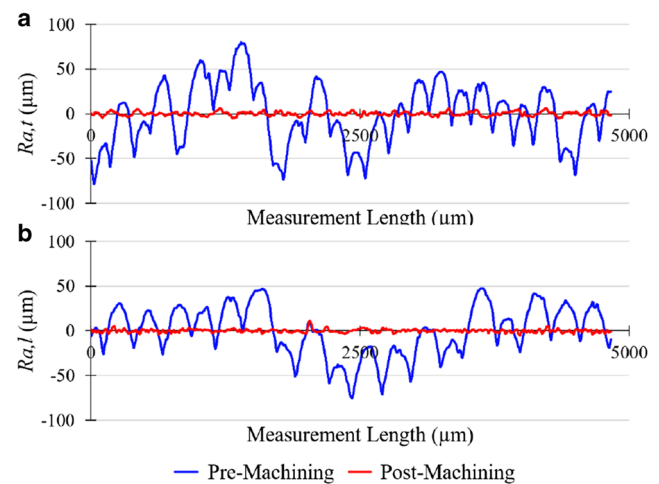
Fig. 12 Roughness profile before and after machining (PA12CF). **a** Longitudinal and **b** transversal

**Fig. 10** Main effects plot for *Ra,l*

Fig. 13 Surface analysis via SEM. **a** Parameter sets 1 and 2. **b** Details of the regions machined with set 1 and **c** set 2
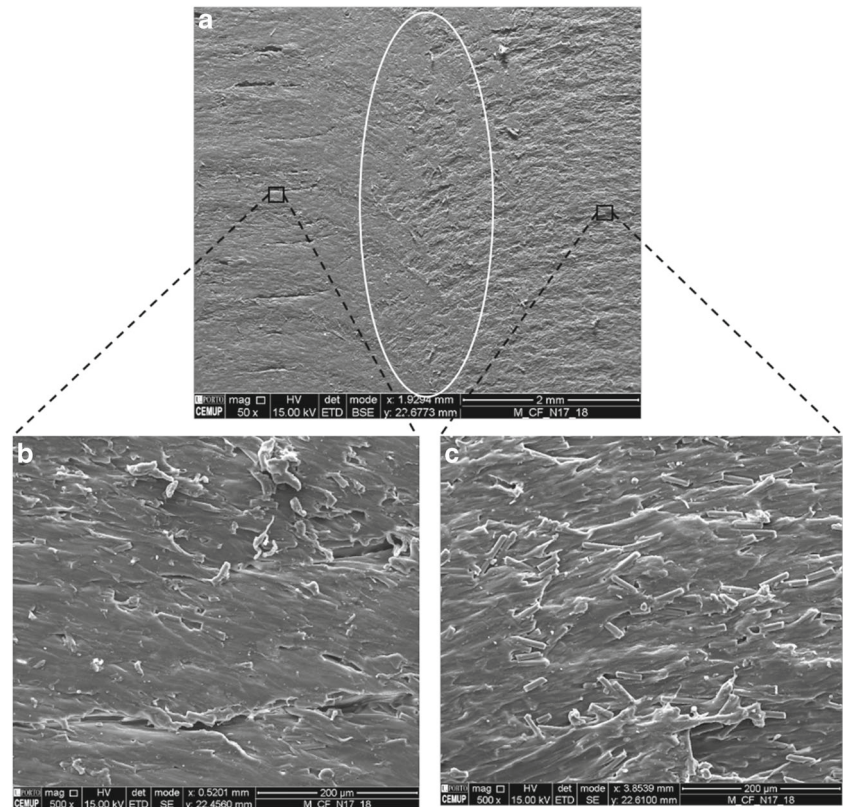
indicating that the matrix polymer was removed and spread throughout the tool path. Figure 13c indicates a higher number of fibres, which are predominantly aligned with the tool rotation direction. This result reinforces the previous hypotheses that the polymer might have overheated at surface level, leaving the fibres broken and reordered.

Tool wear analysis No protocol was taken concerning wear progression analysis; only two different tools were used to perform all the machining tests and the damage was verified in the end. Figure 14 shows the two tools the details of the worn out zone. Considering the two flute tool (Fig. 14a, b), it is possible to observe chipping of the tool edge in

Fig. 14 Tools wear (1st testing approach). **a** Two flute tool, **b** two flute damaged area magnified, **c** detailed of four flute tool and **d** four flute damaged area
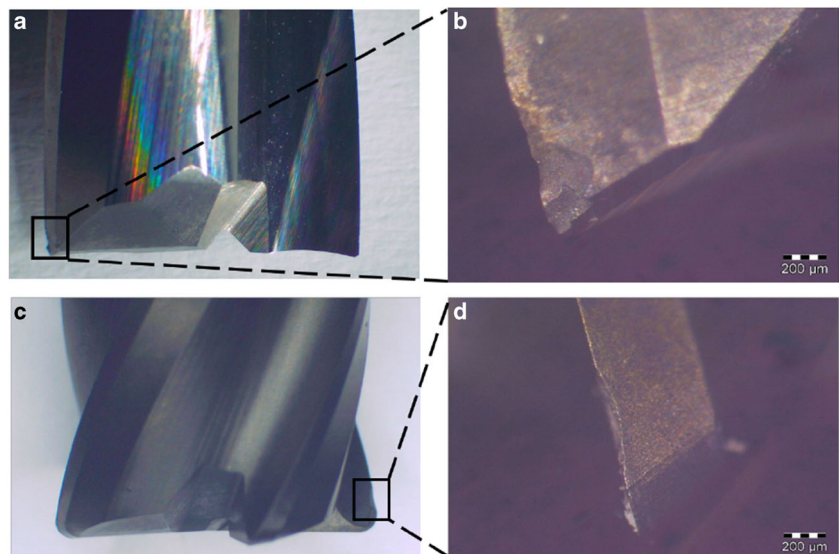
one of the flanks. This type of damage might occur due to several reasons, such as the abrasiveness of the PA12 CF short fibres, a less stable spindle or machine axis and the consequent entrance and exit on the specimen, reasons which, cannot be confirmed with this first approach. Tool wear was found in the four flute tool (Fig. 14c and d) in non advanced state due to its different characteristics (coating and number of flutes), presenting however coating abrasion.

3.1.3 Summary - approach 1

In a general manner, this first approach allowed to demonstrate the possibility of machining FFF parts to improve their surface roughness/dimensional accuracy via CNC machining. An analysis of the material, building orientation, and machining parameters' influence on the overall printed part final surface roughness was performed for this specific subtractive setup. This study was able to indicate some guidelines for the next stage.

Considering the ANOVA analysis, the most influential parameters when taking into account Ra, are the material intrinsic properties, the cutting speed, the type of tool and the feed, thus discarding building orientation and depth of cut. Building orientation was a chosen parameter since machining perpendicularly or parallel to the deposition paths was thought to be a critical parameter. However, being statistically proven non relevant after machining post-processing. The same was considered for the depth of cut, that removing more or less material at each tool pass might not influence the surface roughness.

PA12CF averages lower longitudinal and transverse roughness (1.84 ± 0.11 μm and 2.01 ± 0.34 μm) than its unreinforced version (2.80 ± 0.54 μm and 2.18 ± 0.20 μm), when considering the best combination of parameters (2 flute tool, lower cutting speeds and higher feed), hence leading to the conclusion that the presence of fibres improves the material stiffness, thus improving its machinability in terms of surface finishing.

The two way interactions present an higher level of statistical contribution (51.42% for Ra, t and 47.04% for Ra, l) for the final part finishing than the isolate input variables, since both presented approximately 20% of error.

Material-Tool interaction indicates that PA12 should be machined using a two flute, while for the reinforced material, surface finishing is roughly the same for both tools.

The same cutting speed of 100 m/min is advised for both materials, while higher feeds (0.07 mm/tooth) is advised for better surface finish. This result may be in contradiction with the expected for most metallic materials that show better roughness with reducing the feed. Higher feeds and lower cutting speeds results in less heating, less material softening and less material stir effect. This goes against the literature values, which indicates that lower feeds lead to better surface finishing. It is also shown that improved roughness is obtained with lower cutting speeds, once again contrasting with literature values. In agreement with the literature results is the non-influence of the depth of cut [30].

Tool wear was detected in both tools, namely coating wear in the four flute tool, as well as chipping in the two flutes. This damage was likely caused by the impact in the multiple entries of the tool in the part and due to the presence of abrasive fibres in half of the samples. Outplan CNC machine, was considered as an influential factor, since its structure was susceptible to spindle vibrations during the longitudinal axis travel, which may lead to influenced results. Thus, the need for a newer and more robust hardware would be imperative for this parameter window verification.

SEM analysis showed the presence of a higher number of fibres at the surface for a certain set of parameters. This is caused by the tool edge movement, which allows to conclude that the tool either pulls the fibres out of the polymer or drags them to other zone,s embedding them into the matrix due to the temperature increase resultant of feed and cutting speed. In addition, it is visible that after the machining process, the fibre alignment is perpendicular to the tool advance direction, considering that originally the fibre orientation is the same of the polymer deposition (0, 45 and 90° with the tool trajectory).

In conclusion, the possibility of machining thermoplastic/reinforced with carbon fibre thermoplastics produced by additive manufacture was proven. Finally Table 7 shows the proposed parameters for this specific setup.

3.2 Experimental approach 2

3.2.1 Methods

Considering the conclusions and limitations identified by the first approach, a second experimental plan was conceived. For this test approach, both materials were once again considered, yet studied into separate DOE plans in order to better identify which feature most influences the

Table 7 Optimized processing window for PA12 and PA12CF machining targeting improved finishing - approach 1

| Parameters	PA12		PA12CF	
	Ra,t	Ra,l	Ra,t	Ra,l
Tool type	2 flutes	2 flutes	4 flutes	2 flutes
Cutting speed (m/min)	100	100	100	100
Feed (mm/tooth)	0.07	0.07	0.07	0.07
Building orientation (º)	Non significant			
Depth of cut (mm)	Non significant			
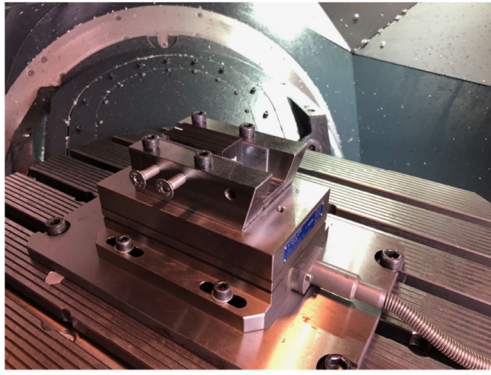
Fig. 15 CNC setup with Kistler multicomponent dynamometer

final result. Since in the first approach, building orientation was statistically non-influential for the final results, it is not considered for this second test programme. As a result, all the samples were printed with the same horizontal orientation. Despite the cutting depth variable being not influencing to the roughness in the first test campaign, it was considered in this second testing programme, since it is a machining parameter (building orientation is not). Thus, this new testing phase will be only focused into machining parameters. To eliminate the possible influence that the subtractive hardware could have on the results, a stiffer and more stable CNC machining centre was used. A tool variable was also kept, being the two flute tool, since it presented the best results in three out of four categories of first test setup (Table 7). Since some unexpected levels of tool wear were found in the first approach, a tool analysis was performed after each machining test. A load cell was added to measure the cutting loads and possibly identify the most critical parameters concerning this approach (Fig. 15).

Subtractive hardware and load cell This second trial was performed on a DMG Mori DMU 60 eVo 5 axis machine,
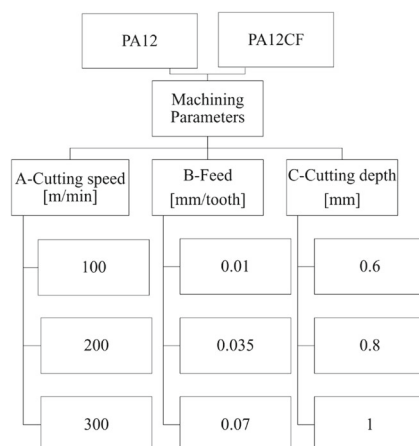
with a working volume of 600x500x500 mm using a similar ER-32 clamping system. Since some tool wear (chipping and abrasion) was found in the first approach, which could be explained by the fibres abrasiveness or due to undesired vibrations found in the first experimental setup, the second approach adopted a stiffer and stabler equipment. The three orthogonal cutting force components were measured with a Kistler multicomponent dynamometer type 9257B connected to a KISTLER 5070A 8-channel amplifier (Switzerland), then transmitted to an Advantech USB 4750A data acquisition card (Taiwan) with a sampling frequency of 4000 Hz. This setup was assembled in the CNC machine as seen in Fig. 15. With this load cell, each milling operation produces a multi component load that will be measured, being the resultant force used as a response in the statistical analysis.

DOE - second test programme A Taguchi DOE was selected in order to minimize the number of printed samples and tools needed to perform the respective tests. As presented in Fig. 16, separated DOE were performed for each material, focusing in machining parameters. A three level DOE was considered, introducing intermediate values for cutting speed and feed, now including higher values for cutting depth than in previous testing programme. A L9 orthogonal array was used accordingly to Taguchi approach for DOE as seen in Table 8. Similarly to the first approach, an ANOVA (with a 95% confidence level) is conducted, determining the most contributive factors. In addition to ANOVA, the main effect plots are presented and, since there are three response levels, post-hoc pairwise comparisons analysis (Tukey HSD and Fisher LSD) are needed to identify the best combination of parameters, for each response type.

Machining parameters Regarding the cutting speed, maximum and minimum values were the same in the primary

Fig. 16 Approach 2 - Taguchi DOE with influential parameters and levels

Table 8 Taguchi L9 orthogonal array of the second testing programme

Condition	Tool	Taguchi L9		
		Cutting speed [m/min]	Feed [mm/tooth]	Depth of cut [mm]
1	1	100	0.010	0.6
2		100	0.035	0.8
3		100	0.070	1
4	2	200	0.010	0.8
5		200	0.035	1
6		200	0.070	0.6
7	3	300	0.010	1
8		300	0.035	0.6
9		300	0.070	0.8

approach, corresponding to 100 and 300 m/min. Since this experiment is a three level Taguchi, an intermediate value of 200 m/min was introduced. The feed procedure included 0.035 mm/tooth as an intermediate value to the extremes of 0.01 and 0.07 mm/tooth. The cutting depths were 0.6, 0.8 and 1.0 mm.

Machining strategy Regarding the first experimental approach, the tool path in each specimen face was divided in two segments, thus allowing to test two different machining parameter combinations (Fig. 6). In this trial (Fig. 17), only one machining parameter set per face is used. The overlap in paths remains at 25%, and the tool starts and finishes the cycle 4 mm outside the sample (laterally). To increase the tool machining time, three faces per specimen were machined with the same parameters.

Tool and wear analysis For this testing procedure, only the flat end two flute 8 mm diameter mill HFMA200820-SOFTLINE, supplied by Palbit, S.A., with an helix angle of 14°, was chosen. Contrarily to the first approach, one tool was used per each cutting speed, three tools in total were used as presented in the Taguchi's array (Table 8). The tool wear was evaluated by through microscopy observation of the cutting edges at the end of each Taguchi experiment condition.

Roughness measurement In addition to transverse and longitudinal Ra measurements, Rz,t and Rz,l were also measured posteriorly to the machining process as shown in Fig. 18 according to ISO 4288 [29]. Rz value is obtained by measuring the vertical distance from the highest to the lowest peak within five sampling lengths, averaging their distances, thus presenting another representative set of data for parameter evaluation. All of these measurements were taken in accordance with the first approach hardware and technique.

3.2.2 Results and discussion - approach 2

Figure 19 depicts the results in terms of Ra,t, Ra,l, Rz,t, Rz,l and cutting loads, obtained for the 9 Taguchi conditions
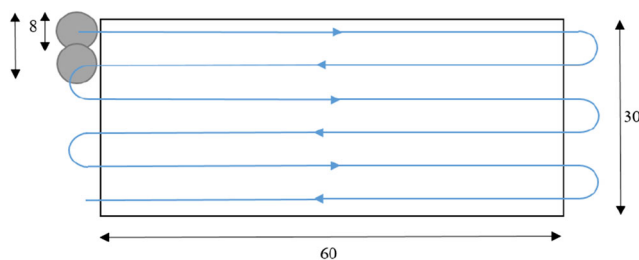

Fig. 17 Tool path strategy for the second programme
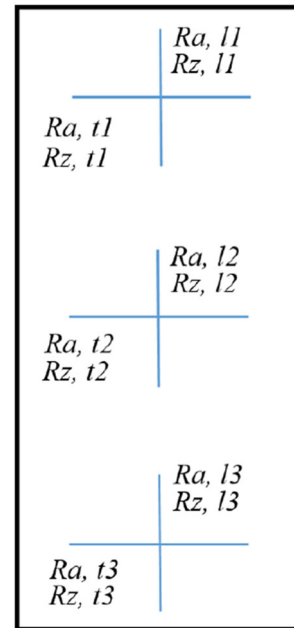

Fig. 18 Measurement points for transversal and longitudinal Ra and Rz

(parameters combinations). It is important to refer that these are average values for each sample/condition of three machined faces. It is possible to observe some preliminary tendencies, even though the most definite results are only presented via main effect plots and ANOVA analysis.
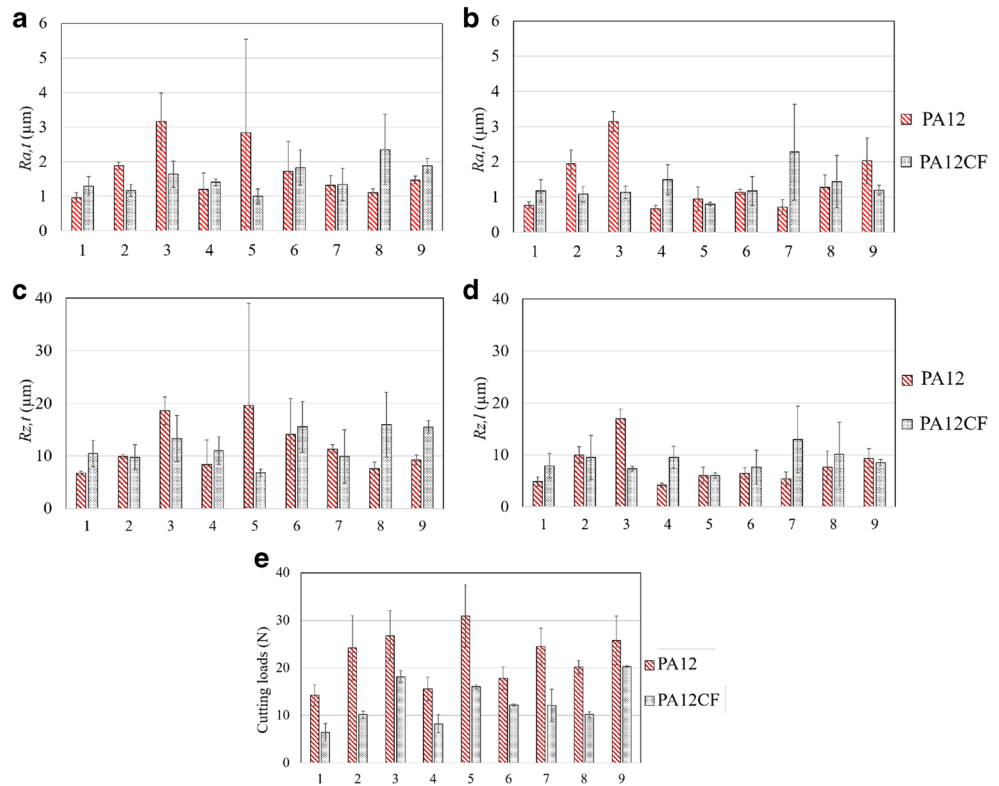
Comparing Ra,l and Ra,t results, it is possible to observe the same trend. Apart from condition 9 (which contradicts the tendency), higher Ra,l values correspond to the higher Ra,t values for the same material. The results show lower PA12 roughness for the 1st, 4th, 6th, 7th, 8th and 9th (only in Ra,t with contrary behaviour in Ra,l) conditions. High standard deviation is also found in Ra,t, PA12, 5th and PA12, 8th condition. Rz values do not present similar tendency as the previous (Ra), showing also high level of deviation in some of the samples.

The most relevant result obtained from this preliminary data analysis is presented in cutting force graph of Fig. 19e. Cutting forces for PA12 are much higher than in the reinforced material for all the conditions, doubling its value for some of the cases. Even though the unreinforced material shows higher deviation/result dispersion, the values are still superior than the forces obtained for PA12CF.

Considering the initial average values obtained for horizontal specimens, the improved results are shown for the conditions that correspond to the best final surface roughness. Since these samples were horizontally printed, longitudinal measurements ($Ra, l/Rz, l$) follow the deposition lines, thus the worst and more significant results are presented in the transversal measurements. It is possible to identify in Table 9 that the improvement in surface

Fig. 19 Taguchi matrix results: **a** *Ra,t*, **b** *Ra,l*, **c** *Rz,t*, **d** *Rz,l* and **e** cutting forces

roughness is 1931% for PA12CF and 2255% for PA12 in the transversal direction, while longitudinally, the increase is 479% and 318% for PA12CF and PA12, respectively. Since final Ra,l and Ra,t present similar results, it is possible to infer that the deposition orientation has no influence on the final surface roughness, agreeing with the data provided by the first approach that discards the building orientation as an influential factor on surface roughness.

According to some findings available in research literature [31, 32], it is claimed that the glass transition temperature (T_g) of a polymer is a crucial parameter concerning surface roughness. This implies that if the temperature of the machining area's surface is higher than

the T_g, a good surface finish is likely to be obtained, since the material is removed in a ductile way. On the other hand, if the temperature is lower, a brittle material removal occurs and a rough surface is obtained. As presented in Table 1 both materials present T_g temperatures of approximately 50°C, that are possible to occur during the machining process, which was conducted without any kind of coolant (dry machining). Since, the reinforced material presents an higher thermal conductivity due to the fibres (Table 1), it could be easier to reach these temperatures than the unreinforced specimens.

ANOVA - second approach Considering that five different responses were obtained for each material, ANOVA analysis was performed. The results are presented, considering that the factors showing no statistically significative influence were disregarded. In addition to ANOVA analysis, the main effect plots are presented, and since there are three response levels, post hoc pairwise comparisons analysis (tukey HSD or fisher LSD) are needed to identify for each response type, the best parameter combination. Therefore, Tukey's test is used to complement ANOVA, in order to find means that are significantly different from each other, i.e. the most influential values of each parameter per response.

The results show that for the reinforced material, no parameters presented acceptable P values for *Ra,l*, *Rz,l*, *Ra,t* and *Rz,l* responses, being the cutting load the only result with statistically influential parameters. For PA12,

Table 9 Improvement factor for machined specimens

PA12CF

	Ra, t (μm)	Ra, l (μm)	Rz, t (μm)	Rz, l (μm)
Pre Machining	19.12±1.96	3.83±0.53	84.58±3.66	19.65±1.87
Machined (C5)	0.99±0.22	0.80±0.05	6.83±0.70	6.04 0.55
Improvement	1931%	479%	1238%	325%

PA12

	Ra, t (μm)	Ra, l (μm)	Rz, t (μm)	Rz, l (μm)
Pre Machining	21.65 ± 2.90	2.45 ± 6.19	84.05±6.07	8.70±0.96
Machined (C1)	0.96±0.14	0.77±0.10	6.75±0.40	4.88±0.88
Improvement	2255%	318%	1245%	178%

Table 10 PA12 *Ra,l* ANOVA (2nd experimental approach)

Source	DF	SS	Contribution	F-Value	P-Value
Cutting speed	2	4.871	26.70%	15.60	0.000
Feed	2	8.67	47.52%	27.76	0.000
Depth of cut	2	1.582	8.67%	5.07	0.017
Error	20	3.123	17.12%		
Total	26	18.246	100.00%		

Fig. 20 PA12 main effect plot for *Ra,l*

similar results were found with non-influential responses in transversal roughness measurements, leaving longitudinal roughness response types and cutting loads to be analysed.

ANOVA analysis for *Ra,l* (Table 10) shows that all three considered inputs are statistically relevant, since an acceptable *p* value is presented. The most contributive set of parameters is the feed with 47.52%, followed by cutting speed (26.70%) and depth of cut (8.67%). As for *Rz,l* (Table 11), all three parameters are also considered influential, thus confirming the previous order with a slight change in the contribution percentages.

Figures 20 and 21 present the main effect plots for both *Ra,l* and *Rz,l*. *Ra,l* is composed by three relevant parameters. Based in Tukeys method, it is possible to say with 95% confidence that for cutting speeds of 200 and 300 m/min statistically similar means are presented, leading to conclude that between them, there is no relevant change in the response, being 100 m/min cutting speed the one that differences from the previous ones. Thus, to obtain better surface roughness (*Ra,l*), higher values of cutting speeds must be selected. Considering the same method for feed parameter, the three chosen values present significantly different means, indicating that 0.070 mm/tooth results in the worst finishing, and 0.010 mm/tooth in the best one, as confirmed by Fig. 20. In the same way, the depth of cut of 0.6 mm is the only significantly different mean, resulting in the best values of roughness, while 0.8 and 1.0 mm have statistically identical means, resulting in similar roughness results. When considering *Rz,l*, the behaviour is similar to *Ra,l* except for the depth of cut, where there is an overlap in the terms, thus making it impossible to make an adequate conclusion using Tukey, Fisher or other pairwise comparisons.

Cutting loads PA12 cutting loads ANOVA analysis in Table 12 shows that the cutting speed was not statistically significant, since it was outside the confidence interval. Depth of cut presents 40.97% of the contribution in the final values, while feed is 21.82%. For PA12CF, as depicted in Table 13, all parameters are to be considered as equally influential. Depth of cut and feed defines the chip section, which leads to more or less proportional increase in the cutting loads.

Figures 22 and 23 present the main effect plots for cutting forces measured for both materials. Analysing PA12 first and basing these results on the Tukey's method it is possible to say with 95% confidence that higher feeds (0.070 and 0.035 mm/tooth) mean similar results, leading to conclude that there is no significant difference between them. As such, 0.010 mm/tooth is confirmed as the value that creates lower cutting forces as seen in Fig. 22. The same methodology is used to understand the depth of cut results, indicating that 0.6 and 0.8 mm have similar means, leading both to identical lower cutting forces. On the other hand, the difference in means indicates that 1.0 mm cutting depth creates a significant increase in cutting forces, as presented in Fig. 22. With regards to the reinforced material (PA12CF), the same overlap in the terms is encountered for the cutting speeds. As such, it is

Table 11 PA12 *Rz,l* ANOVA (2nd experimental approach)

Source	DF	SS	Contribution	F-Value	P-Value
Cutting speed	2	117.53	27.86%	12.75	0.000
Feed	2	167.63	39.74%	18.18	0.000
Depth of cut	2	44.44	10.54%	4.82	0.020
Error	20	92.2	21.86%		
Total	26	421.8	100.00%		
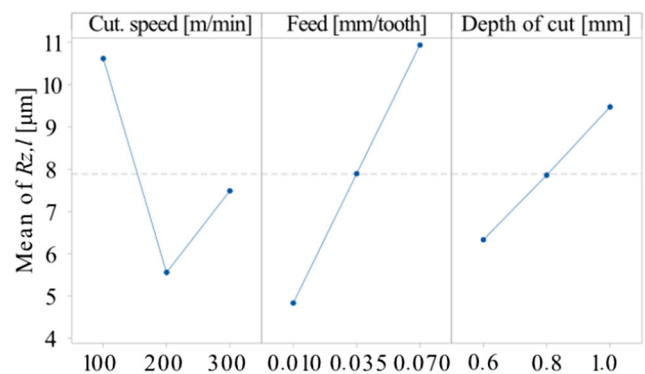
Fig. 21 PA12 main effect plot for *Rz,l*

Table 12 PA12 cutting loads ANOVA (2nd experimental approach)

| Source	DF	SS	Contribution	F-Value	P-Value
Feed	2	239.63	21.82%	6.45	0.006
Depth of cut	2	450.07	40.97%	12.11	0.000
Error	22	408.77	37.21%		
Total	26	1098.47	100.00%		

not possible to make adequate conclusions using Tukey's pairwise comparison. However, through Fisher LSD, and using the same 95% confidence level, it is possible to infer that in this case 100 and 200 m/min have similar mean values, thus presenting no considerable difference in cutting force. 300 m/min presents a significantly different value, resulting in a considerable difference in results. This means that, in order to create lower cutting forces, 100 or 200 m/min should be used. Considering feed and cutting speed, Tukey's method was successfully applied, presenting significantly different means for all the cases, leading to conclude that every feed/depth of cut increment has effect, being exactly portrayed by the main effect plot in Fig. 23.

Tool wear analysis Microscopic analysis was performed after the machining process for each Taguchi condition. Tables 14 and 15 show tool surfaces after conditions 3, 6 and 9, which correspond to the last usage of that tool for a specified cutting speed. Considering the parameters combinations, at the end of the 3rd condition (tool 1 - the tool has been subjected to the milling operation for 19 min and 32 s in 3 samples, 3 faces each). At the end of the sixth condition (second tool - the tool has milled during 9 min and 58 s), while for the third tool at the end of condition 9, the tool was used 6 min and 27 s. The presentation of only these final conditions was considered for the sake of conciseness. However, considering the results obtained, all of the conditions are discussed.

Regarding the unreinforced material, and following the same logic of the tables, microscopic observations show that, for the first condition, an abrasion is notorious in the cutting edge 1 and a small crater wear in edge 2. For condition number 2, the abrasion in cutting edge 1 is roughly the same. In the edge 2, beyond the crater wear,

Table 13 PA12CF cutting loads ANOVA (2nd experimental approach)

| Source	DF	SS	Contribution	F-Value	P-Value
Cutting speed	2	33.66	6.08%	4.25	0.029
Feed	2	288.17	52.02%	36.39	0.000
Depth of cut	2	152.9	27.60%	19.31	0.000
Error	20	79.19	14.30%		
Total	26	553.93	100.00%		
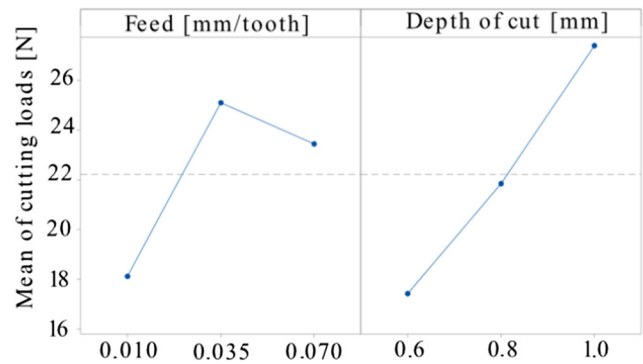
Fig. 22 PA12 main effect plot for cutting forces

abrasion is now also visible along the edge for roughly 1 mm. The third condition shows an increase abrasion wear in both edges. At the end of the first condition of the second tool (condition number 4), chipping in cutting edges number 1 and 2 is notorious, a damage that was aggravated along the following two conditions, as presented in (C6) Table 14. The third tool showed some abrasion in cutting edge 1 and chipping in edge 2 after the 7th condition, which was not significantly increased by the following two conditions, as seen in condition 9 images.

Microscopical analysis of the tools used for the reinforced material depict a different behaviour with little to no damage (see images in Table 15). For the initial three conditions, the result is similar, presenting some abrasion wear in both cutting edges but no serious damage. The same result is found for the second tool, showing no signs of damage, even in the sixth condition. Condition number seven presents chipping in cutting edge 1 and 2, with the edge vertex missed. With test number 8, the damage seems to be accentuated for both edges, while also presenting an increased chipping area. Final condition shows an increase in the chipping area for edge 1 and a complete wear due to abrasiveness of the vertex in the second edge, as can be seen in Table 15.

By relating the tool wear analysis results with the cutting loads, it is possible to understand that the higher loads
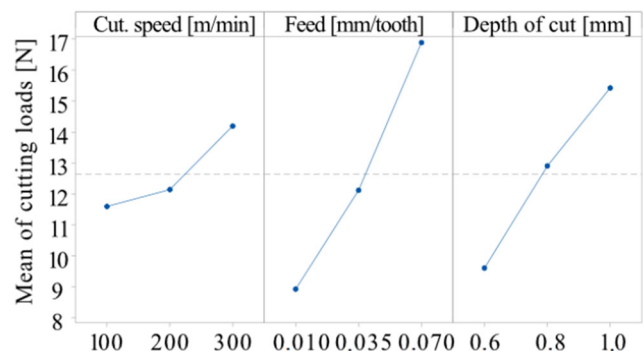
Fig. 23 PA12CF main effect plot for cutting forces

**Table 14** Wear analysis for PA12 tools (40x magnification), 2nd testing approach

Condition	Cutting edge 1	Cutting edge 2	Lateral view
3			
6			
9			1mm
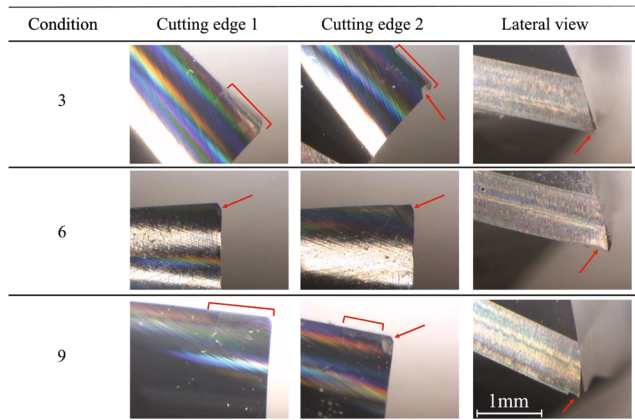
generated by machining increased the wear of the tool used in the unreinforced material.

3.2.3 Summary - approach 2

This second approach allowed a deeper approximation to the machining parameter question. In addition, testing these parameters in a more precise and stable machine was a way of validating their application to different types of machines. As a consequence of the first approach, an higher number of responses was studied to better understand the material and tool behaviour. Taking into account the previous results, the following remarks were drawn:

Considering the five types of responses studied for each material, only cutting forces (for both materials) and the longitudinal roughness Ra,l and Rz,l for PA12 were statistically relevant, with at least one parameter contradicting the null hypotheses (P value$<$ 95%). For PA12CF, Ra,l and Ra,t present an average value of 1.30±0.41 μm,

Table 15 Wear analysis for PA12CF tools (40x magnification), 2nd testing approach

Condition	Cutting edge 1	Cutting edge 2	Lateral view
3			
6			
9			1mm
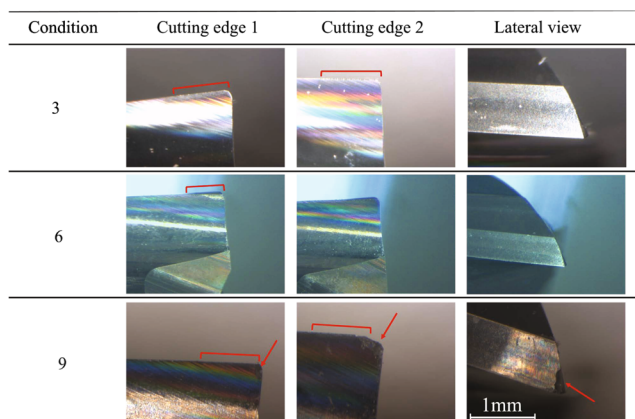
Table 16 Optimized processing window for PA12 and PA12CF machining targeting improved finishing - approach 2

Parameters	PA12CF	PA12		
	Cutting Force	Ra, l	Rz, l	Cutting Force
Cutting speed [m/min]	100/200	200/300	200/300	Non Significant
Feed [mm/tooth]	0.010	0.010	0.010	0.010
Depth of cut [mm]	0.6	0.6	–	0.6/0.8

in the 9 tests and 1.54±0.42 μm respectively, while PA12 presents 1.40±0.82 μm and 1.74±0.77 μm. It is possible to confirm that PA12CF presents a lower average, but also a lower standard deviation. This lower deviation, can relate to the fact that the parameter combinations present lower influence on the PA12CF, thus the lack of statistically contributive results, and consequently easier machining.

Through the ANOVA performed for PA12's Ra,l and Rz,l, it was possible to conclude that there is an agreement in the contributions, being the most significant parameter the feed, with 47.52% and 39.74%, respectively, followed by the cutting speed (26.70% and 27.86%) and the depth of cut (8.67% and 10.54%).

Considering Ra, l and Ra, t similar results (Table 9), it is possible to confirm that printing orientation is not an influential.

Considering the tool machining time, it is noticeable that for tool number 1 it is used more than double the time of tool number 2, and the triple of number 3, although it is not notorious a significant damage among the tools for PA12. On the contrary, PA12-tool 3 presents high abrasion wear levels and chipping that are not found in the first tool. This leads to the conclusion that there is no direct relationship between the machining time and tool wear for these specific approaches.

The analysis of the cutting loads showed that PA12CF values were much lower than for PA12, which reinforces the previous statement that PA12CF is easier to machine. In addition, microscope observations shows much faster/higher levels of tool wear in the ones used to machine the unreinforced samples.

Table 16 presents a synthesis of the optimal parameters advised to machine this type of materials with this specific setup.

4 Conclusions

This work intended to understand how PA12 based material printed parts behave in machining operations and what

are the main influential factors, by defining a parameter operation window for surface analysis. Two subsequent experimental approaches were performed, showing different, but prominent results creating as such a progress towards hybrid manufacturing. While this first machining process was performed in less stiff/precise machine-tool, the second approach had its focus in exploring the best set of conditions in a more stiff precise machine. The results show that the purposed parameters combination for the first machine tool behave differently in the second hardware. As a consequence, results in Tables 7 and 16 are different.

First approach ANOVA analysis proved that the building orientation influence was not relevant for the final surface roughness. Even though being a discarded parameter for the second test, this could be proved once again, since final Ra, l and Ra, t are similar for both materials in a longitudinal sample (0.80±0.05 vs 0.99±0.22 for PA12CF and 0.96±0.14 vs 0.77±0.10 for PA12).

In the first approach, the feed variable had contributions of 2.79% (Ra, t) and 10.68% (Ra, l), while with interactions the influence was over 30% for both cases. For the second approach, only PA12 presented significative values for surface roughness, yet, it is possible to observe that in this case the feed presented a 47.52% contribution. Thus, it can be concluded that feed rate is influential on surface roughness. As far as depth of cut, in the first approach it was not considered as a statistically relevant parameter. However, through the second approach, it is possible to perceive that this value influences on the PA12 material's final roughness. In addition, the PA12 and PA12CF cutting depth presented a contribution of 40.97% and 27.60% for the respective cutting forces generated, which is a surprising result since carbon fibres despite producing material reinforcement, their effects on machinability is not negative. It is also shown that for the same cutting depth, higher forces are exhibited by the unreinforced material, which justifies the higher levels of damage found in the tools used in this material. Since tool wear (abrasion and chipping) was found in both approaches, the initial idea that the damage was created due to the hardware's lack of stiffness is discarded.

The second approach also implied that the best combination of parameters was different for both materials, yet reaching similar final material roughness. Since none of the inputs revealed to be statistically contributive for PA12CF, it is possible to affirm that the variation of parameters is less influential on the final result. This might occur due to higher machining temperatures created by the presence of fibres. The difference in parameter results considering both approaches is attributed to the machining hardware, leading to conclude, that the suggested parameters will vary with the type of hardware used.

In conclusion, it was proven that FFF PA12 and PA12CF printed parts can be machined to improve their final surface finishing, resulting in a roughness (Ra, t) decrease of 2255% and 1931% respectively.

Finally, this type of testing is essential for the development of a hybrid process, leading to conclude from both approaches to the problem that machining hardware is as crucial as the material to be machined.

References

1. ISO/ASTM: ISO ASTM 52900:2015 - Additive manufacturing - General principles - Terminology (2015)
2. Williams G, Trask R, Bond I (2007) A self-healing carbon fibre reinforced polymer for aerospace applications. Compos Part A: Appl Sci Manuf 38(6):1525–1532
3. Chun LM, Kowalik M (2018) Preliminary studies for alternative lattice core design for FDM 3D printed sandwich panels. Mater Today: Proc 5(13):26519–26525
4. Mayyas A, Qattawi A, Omar M, Shan D (2012) Design for sustainability in automotive industry: a comprehensive review. Renew Sust Energy Rev 16(4):1845–1862
5. Ullah H, Harland AR, Silberschmidt VV (2015) Dynamic bending behaviour of woven composites for sports products: experiments and damage analysis. Mater Des 88:149–156
6. Singh D, Singh R, Boparai KS (2018) Development and surface improvement of FDM pattern based investment casting of biomedical implants: a state of art review. J Manuf Process 31:80–95
7. Singh R, Singh S, Singh IP, Fabbrocino F, Fraternali F (2017) Investigation for surface finish improvement of FDM parts by vapor smoothing process. Compos Part B: Eng 111:228–234
8. Zhang Y, Chou K (2008) A parametric study of part distortions in fused deposition modelling using three-dimensional finite element analysis. Proc Institut Mech Eng Part B: J Eng Manuf 222(8):959–967
9. Santana L, Alves JL, da Costa Sabino Netto A (2017) A study of parametric calibration for low cost 3D printing: seeking improvement in dimensional quality. Mater Des 135:159–172
10. Sood AK, Ohdar RK, Mahapatra SS (2009) Improving dimensional accuracy of Fused Deposition Modelling processed part using grey Taguchi method. Mater Des 30(10):4243–4252
11. Peng A, Xiao X, Yue R (2014) Process parameter optimization for fused deposition modeling using response surface methodology combined with fuzzy inference system. Int J Adv Manuf Technol 73(1–4):87–100
12. Galantucci LM, Lavecchia F, Percoco G (2009) Experimental study aiming to enhance the surface finish of fused deposition modeled parts. CIRP Ann Manuf Technol 58(1):189–192
13. Lalehpour A, Barari A (2016) Post processing for fused deposition modeling parts with acetone vapour bath. IFAC-PapersOnLine 49(31):42–48
14. Singh J, Singh R, Singh H (2016) Repeatability of linear and radial dimension of ABS replicas fabricated by fused deposition

modelling and chemical vapor smoothing process: a case study. Measur: J Int Measur Confederation 94:5–11

15. Amanullah AN, Murshiduzzaman M, Saleh T, Khan R (2017) Design and development of a hybrid machine combining rapid prototyping and CNC milling operation. Procedia Eng 184:163–170

16. Lee WC, Wei CC, Chung SC (2014) Development of a hybrid rapid prototyping system using low-cost fused deposition modeling and five-axis machining. J Mater Process Technol 214(11):2366–2374

17. Boschetto A, Bottini L, Veniali F (2016) Finishing of fused deposition modeling parts by CNC machining. Robot Comput Integr Manuf 41:92–101

18. Tomal ANMA, Saleh T, Khan MR (2018) Combination of fused deposition modelling with abrasive milling for attaining higher dimensional accuracy and better surface finish. IIUM Eng J 19(2):221–231. cited By 0

19. Kara F (2017) Taguchi optimization of surface roughness and flank wear during the turning of DIN 1.2344 tool steel Materialpruefung/Materials Testing

20. Kara F, Öztürk B (2019) Comparison and optimization of PVD and CVD method on surface roughness and flank wear in hard-machining of DIN 1.2738 mold steel. Sens Rev 39(1):24–33

21. Karabatak M, Kara F (2016) Experimental optimization of surface roughness in hard turning of AISI D2 cold work tool steel. J Polytechnic-Politeknik Dergisi 19(3):349–355

22. Parzlich s.r.o. Fillamentum Nylon FX256 Material Datasheet

23. Parzlich s.r.o. Fillamentum Nylon CF15 Carbon Material Datasheet

24. Fonseca J, Ferreira IA, De Moura MFSF, Machado M, Alves JL (2019) Study of the interlaminar fracture under mode I loading on FFF printed parts. Compos Struct 214:316–324

25. Vasile G, Fetecau C, Serban A (2014) Experimental research on the roughness of surfaces processed through milling polyamide composites. Materiale Plastice 1(2):205–212

26. Izamshah R, Azam MA, Hadzley M, Ali MA, Kasim MS, Abdul MS (2013) Study of surface roughness on milling unfilled-polyetheretherketones engineering plastics. Procedia Eng 68:654–660

27. Bozdemir M, Aykut Ş (2012) Optimization of surface roughness in end milling Castamide. Int J Adv Manuf Technol, 495–503

28. Voss R, If TD, Seeholzer L, Kuster F, Wegener K (2017) CIRP Journal of Manufacturing Science and Technology Influence of fibre orientation, tool geometry and process parameters on surface quality in milling of CFRP. CIRP J Manuf Sci Technol 18:75–91

29. ISO. ISO 4288 - Geometrical Product Specifications (GPS) – Surface texture: Profile method – Rules and procedures for the assessment of surface texture (1996)

30. Alauddin M, Choudhury IA, El Baradie MA, Hashmi MSJ (1995) Plastics and their machining: a review. J Mater Process Tech 54(1-4):40–46

31. Smith EF (1989) Single-point turning of amorphous thermoplastic polymers. North Carolina State University, PhD thesis

32. Xiao KQ, Zhang LC (2002) The role of viscous deformation in the machining of polymers. Int J Mech Sci 44(11):2317–2336

Affiliations

Isaac Ferreira[1,2] (ID) · **Rui Madureira[1]** · **Santiago Villa[1]** (ID) · **Abílio de Jesus[1,2]** (ID) ·
Margarida Machado[2] (ID) · **Jorge Lino Alves[1,2]** (ID)

Rui Madureira
rdmadureira@inegi.up.pt

Santiago Villa
svilla@inegi.up.pt

Abílio de Jesus
ajesus@fe.up.pt

Margarida Machado
mmachado@inegi.up.pt

Jorge Lino Alves
falves@fe.up.pt

[1] Faculdade de Engenharia, Universidade do Porto, Rua doutor Roberto Frias 400, Porto, Portugal

[2] INEGI, Rua doutor Roberto Frias 400, Porto, Portugal